ANCHORAGE REQUIREMENTS OF DEFORMED BARS IN GROUTED MASONRY

Tariq S. Cheema[I] and Richard E. Klingner[II]

SYNOPSIS

Anchorages of Grade 60 (f_y = 60000 psi) deformed reinforcing bars in grouted concrete masonry were tested under monotonically increasing tensile loads. A total of 78 tests were conducted on bar sizes #4, #8, and #11. Observed failure modes were clearly influenced by the non-homogeneous nature of concrete masonry. The bar diameter had a significant effect on behavior and cracking mechanisms. Test data indicated that the current recommendations of the U.S. Uniform Building Code [1] provide a decreased factor of safety for larger size bars as compared to smaller ones.

INTRODUCTION

The development of rational design methods for masonry structures has led to an increased use of reinforced concrete masonry load-bearing walls for buildings in seismic areas. These walls are commonly single-wythe, constructed in running bond from hollow-core concrete blocks. Reinforcing bars are placed vertically in the block cores at a typical spacing of 36 in. or less. In general, all the cores in the wall are filled with a high slump pea-gravel concrete mix, commonly called grout.

The effectiveness of the reinforcement depends on the bond stress that can be developed between the deformed bars and the grout. Modern codes express the available bond strength in terms of minimum required development length or an equivalent average bond stress. The current United States Uniform Building Code [1] specifies an allowable bond stress of 140 psi for bars of all sizes in inspected construction. Figure 1 presents the anchorage length requirements of the Uniform Building Code [1] and also compares them to ACI 318-77 Building Code [2] criteria for reinforced concrete having f'_c = 3000 psi, a lower bound to the cylinder strength of typical grout.

The main objective of this research was to evaluate the adequacy of the anchorage requirements of the Uniform Building Code [1]. Other objectives were to determine the parameters governing bond strength in grouted concrete masonry walls, to identify anchorage failure mechanisms, and to develop failure models through analytical studies. Due to space limitations, this paper will discuss the principal experimental results only.

TEST PROGRAM

To develop understanding of failure mechanisms for a broad range of potential applications, bar sizes #4, #8, and #11 were selected for anchorage tests. As shown in Fig. 2, test specimens consisted of single-wythe walls constructed from 8"×8"×16" hollow two-core concrete blocks. The walls were 88 in. long and their height was governed by the test length of

[I] Graduate Student, Civil Engineering, U. of Texas, Austin, Texas, U.S.A.

[II] Asst. Professor, Civil Engineering, U. of Texas, Austin, Texas, U.S.A.

the anchorages in each wall. The construction utilized one type of block and mortar. Horizontal reinforcement of both ladder and truss types was placed in mortar bed joints at 16" intervals. The test program was divided into two series, each utilizing a different grout mix. Due to space requirements, only the results of the second series involving 42 tests are described here. Table 1 describes those anchorages, and Table 2 presents the mechanical characteristics of the materials used.

TABLE 1 DESCRIPTION OF ANCHORAGES IN SERIES II

Bar Size	Anchorage Length, in.	No. of Tests	Wall Height, in.
#4	5	3	24
	10	4	24
	15	4	24
	21	6	24
#8	20	4	24
	28	4	32
	43	6	48
#11	29	3	32
	39	4	40
	59	4	64

TABLE 2 MECHANICAL CHARACTERISTICS OF MATERIALS USED
(Mix proportions are by volume)

Material	Specimen	Average 28 day strength	Description
Block	8"x8"x16" two-core units	1400 psi on net area	Lightweight aggregate
Mortar	2" cubes, 3"x6" cylinder	1800 psi	1 cement:1/2 lime: 4-1/2 sand
Grout	3"x3"x6"	3500 psi	1 cement:4.4 sand:2.4 gravel Max. aggregate size = 3/8" 11" slump
Grouted Prisms	8"x16"x16"	1980 psi	

TEST SETUP

Pullout force on the bars was applied by a centerhole actuator. Previous pullout tests [3] had indicated that if the actuator reacted directly on the wall near the bar, concentrated compressive stresses near the loaded end of the anchorage could result in unrealistically high values of observed bond stress. To reduce this effect, a steel beam supported the the hydraulic actuator and transferred its load to the wall at two locations away from the bar being tested. Based on elastic finite element solutions, the distance between the bar and the reactions was set at 12" for the #4 bars, 18" for the #8 bars, and 24" for the #11 bars. The eccentricity between the pullout force and the reactions on the wall causes an overall moment on the wall portion within the reaction span. A finite element study showed this moment would produce tensile stresses at the top of the wall in excess of the estimated tensile strength of the masonry, leading to a premature failure of the specimen. Using a second hydraulic actuator, eccentric lateral compression was therefore applied to the specimen to reduce these tensile stresses to acceptable values. Figure 2 presents a schematic drawing of the test setup.

Test data included load in the bar, lateral compression applied to the wall, strains at various locations on the bar, and the slip of the bar relative to the masonry at locations along each bar. Loads were calculated using load cells positioned under the hydraulic actuators, and also using pressure transducers connected to the actuators. Strain in the bars was calculated using surface bonded SR-4 paper gages. Slip of the bar relative to the masonry was measured using slip wires [4].

FAILURE CRITERION FOR ANCHORAGES

Anchorage failure was assumed to have occurred at a tail-end slip of 0.0005 in. While somewhat conservative, this criterion was adopted to account for the effects of lateral compressive stresses caused by the combined loading applied to the wall. Figure 3 shows a typical lateral stress distribution determined analytically assuming linear elastic behavior. This investigation tested several anchorages which were identical except for the computed average lateral compressive stresses. Those anchorages having stresses of 100 psi failed immediately at the first indication of tail-end slip. Otherwise identical anchorages with higher lateral stresses began to show tail-end slip at comparable load levels, but did not fail until reaching load levels about 20% higher. It was concluded that this gradual failure behavior was due to the effect of lateral stresses, and that the anchorages would have failed at the first tail-end slip had those stresses been lower. To have a criterion which would be independent of average lateral stress, failure was defined as occurring at a tail-end slip of 0.0005 in.

TEST RESULTS

#4 Bars--The bars were loaded in 1-kip increments. The first lead-end slip was usually recorded at 4-kip loads. All anchorages with 15" and 21" embedment lengths reached the yield load of 13 kips. No cracks were observed, and zero tail-end slip was noted in these tests. Figure 4 shows the variations of load and slip along the length of a typical bar with 15" embedment length. At yield, most of the load is transferred by the lead 10" length of the bar, by approximately uniform bond stress. Slip has progressed to the middle of the bar. Anchorages with 10" embedment length were also able to reach the yield load of 13 kips without observable cracking. However, these bars recorded tail-end slip values of 0.0005" or more at yield, implying failure as noted above. Bars with 5" embedment length failed at an average load of 8 kips, corresponding a bar stress of 40 ksi. The failure mode was shearing of the grout around the bar perimeter, commonly referred to as "pullout".

Figure 5 presents the observed capacity as a function of anchorage length for the #4 bars. Test data indicate that an embedment of 11" is sufficient to develop the yield strength of the #4 bars, while the UBC recommends a development length of 21". In that sense, the UBC recommendation has an overall factor of safety of 21/11, or 1.9.

#8 Bars--The load was applied in 4-kip increments up to 20 kips, and in 2-kip increments for loads above 20 kips. All anchorages with 43" embedment length reached the yield load of 51 kips without tail-end slip. All four anchorages with 28" embedment failed before reaching the yield load. Their average capacity was 46 kips. Figure 6 shows the variation of load and slip along the length of a typical #8 bar with 28" embedment length. Near failure, the bond stress is greatest near the tail end of the bar, while the slip is approximately linear over the embedment length. All bars with 20" embedment length failed at an average load of 38 kips, corresponding a bar stress of 48 ksi.

As shown in Fig. 7, extensive cracking was observed for #8 anchorages that failed to develop yield capacity. In most cases, the cracking began at a bar stress of $0.4f_y$, in the form of a vertical splitting crack at the loaded end. A horizontal crack in the top mortar joint was the next damage observed. As the pullout force increased, the splitting crack progressed down the length of the rebar and additional horizontal cracks appeared in the lower bed joints. The bed joint cracks propagated along the face of the wall on a diagonal, forming a flat V-shape. At ultimate, the face shell of the loaded-end block spalled off, and the horizontal crack in the top bed joint propagated to the bearing reactions by taking a diagonal path through the top blocks. Radial cracks were observed in the grout core at the loaded end of the bar.

Figure 8 shows the capacity of #8 anchorages for various embedded lengths. Test data indicate that the embedment required to develop the yield strength of #8 bars is approximately 33", compared to the UBC [1] recommendation of 43". This implies an overall factor of safety of 1.3.

#11 Bars--The bars were loaded in 5-kip increments. The first lead-end slip was usually recorded at 10-kip loads. All anchorages with 59" embedment length developed the yield load of 102 kips without tail slip. Of the four bars with 39" embedment, two reached the yield load while the other two failed at a load of 95 kips. Figure 9 presents the variations of load and slip along a 39" anchorage that failed before reaching yield. Near failure, almost no load is transferred to the wall over the first third of the anchorage, and slip has progressed to the tail end in an approximately linear variation. All three bars with 29" embedment failed at an average load of 74 kips.

Figure 10 shows the crack pattern associated with a typical #11 bar. Horizontal cracking in the top mortar bed joints is the first damage in the wall. A vertical crack in the head joint nearest to the test bar appears next. As the load is increased, the head joint crack joins the bed joint crack at the corner of the block. This pattern is followed in the underlying masonry courses. The bed cracks propagate diagonally along the face of the wall to form a flat V-shape similar to the cracking observed in tests on #8 bars. The vertical splitting cracks are restricted to the loaded-end block only.

Figure 11 presents the capacity of #11 anchorages for various embedment lengths. Test data indicate that approximately 45" of embedment is required to develop yield load, compared to the UBC [1] recommendation of 59". This implies an overall factor of safety of 1.3.

INTERPRETATION OF RESULTS

Test results show that the UBC [1] recommendations for the anchorage length of bars in grouted concrete masonry do not provide a uniform factor of safety for all bar sizes. The overall factor of safety is about 1.9 for #4 bars, but only about 1.3 for #8 and #11 bars. While this variation is significant in itself, it is also important to relate anchorage requirements to the actual anchorage behavior of grouted masonry as distinguished from concrete.

Preliminary analysis of failure patterns suggests that although the anchorage behavior of deformed bars in grouted concrete masonry is similar to concrete in some respects, it is very different in others. In a manner analogous to that of concrete, the anchorage behavior of grouted masonry depends on the bond-slip behavior of the bars and grout, and on the resistance of the grout to splitting. However, it also seems to depend on the confining effect of the blocks in preventing splitting of the grout core, and on the resistance of the horizontal and vertical mortar joints in preventing liftoff of a block or group of blocks. Evidence for these hypotheses is provided by contrasting the failure patterns for the three bar sizes tested.

Those #4 bars having insufficient anchorage length failed by simple pullout. They were unable to develop sufficient bond force to resist yield loads in the bars. At that load level, they were unable to develop a sufficient radial force to split the grout, and also unable to develop sufficient bond force to lift the lead-end block. As a result, no cracks were observed for this bar size.

On the other hand, those #8 and #11 bars having insufficient anchorage length appeared to fail by a combination of splitting and liftoff. The liftoff mechanism, indicated by the presence of cracks in the horizontal mortar joints, is particularly evident for the #11 bars. As shown in Fig. 10, the horizontal mortar cracks either join vertical mortar cracks or propagate diagonally to the top edge of the wall, effectively disconnecting the upper layer of blocks from the rest of the wall. This greatly reduces the anchorage provided at the lead end of the bar. Figure 9 shows the nearly uniform bar tension over the first third of the #11 anchorage at failure, implying negligible anchorage over that portion of the bar. The failures observed for #8 and #11 bars suggest that the capacity of such larger-diameter bars may be governed by resistance to liftoff rather than pullout. Liftoff is due to the presence of regularly spaced planes of weakness perpendicular to the direction of anchorage, a condition peculiar to grouted masonry as distinguished from concrete. Based on these preliminary failure hypotheses, it is believed that caution should be used in applying concrete anchorage data to grouted masonry, particularly where larger-size bars are concerned.

CONCLUSIONS

1. UBC [1] recommendations for anchorage lengths of deformed bars in grouted masonry do not provide a uniform overall factor of safety. The recommendations are less conservative for #8 and #11 bars than for #4 bars.
2. Inadequately anchored #4 bars failed by pullout due to exceedance of available bond capacity. Inadequately anchored #8 and #11 bars failed by a combination of longitudinal splitting, and liftoff of blocks along horizontal mortar joints. Because this liftoff failure mechanism is peculiar to anchorages in masonry, caution is suggested in designing masonry anchorages using data obtained in anchorage tests on concrete.
3. Further experimental and analytical research is needed to clarify mechanisms of anchorage failure in grouted masonry, and to suggest appropriate design procedures.

ACKNOWLEDGMENT

The authors are grateful to the Bureau of Engineering Research at The University of Texas at Austin, U.S.A., for the financial support of this project.

UNITS

1" = 1 in. = 25.4 mm
1k = 1 kip = 4.448 kN
1 psi = 0.006895 MPa
1 ksi = 6.895 MPa

REFERENCES

1. Uniform Building Code, 1976 Edition, International Conference of Building Officials, California, U.S.A.

2. ACI Standard 318-77, "Building Code Requirements for Reinforced Concrete," American Concrete Institute, Detroit, Michigan, U.S.A., 1977.

3. "Bond Stress--The State of the Art," Report by ACI Committee 408, ACI Journal, V. 63, No. 11, November 1966, pp. 1161-1190.

4. Minor, J., and Jirsa, J., "Behavior of Bent Bar Anchorages," ACI Journal, V. 72, April 1975, pp. 141-149.

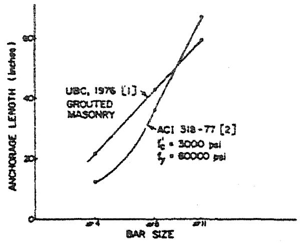

ANCHORAGE REQUIREMENTS FOR DEFORMED BARS

Fig. 1

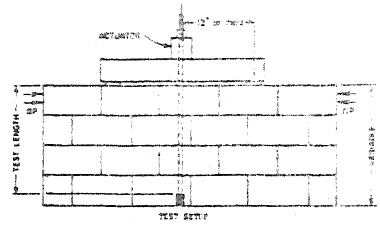

TEST SETUP

Fig. 2

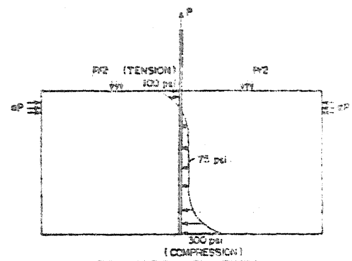

Fig. 3

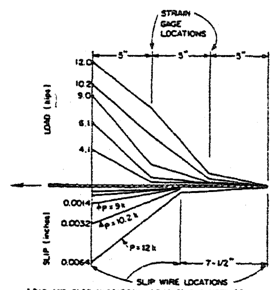

LOAD AND SLIP VARIATION ALONG #4 BAR WITH 15-in. ANCHORAGE

Fig. 4

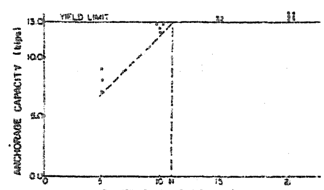

ANCHORAGE CAPACITIES OF #4 BARS

Fig. 5

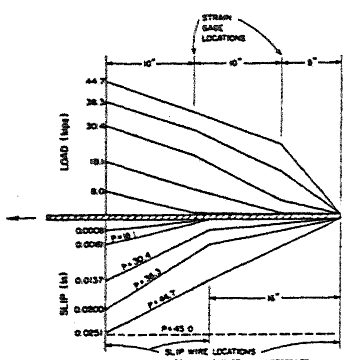

LOAD AND SLIP VARIATION ALONG #8 BAR WITH 28-in. ANCHORAGE

Fig. 6

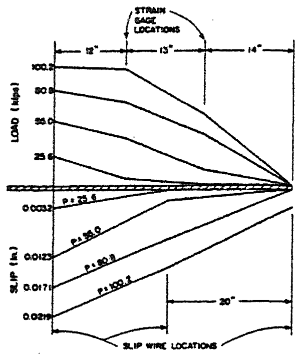

LOAD AND SLIP VARIATION ALONG #11 BAR WITH 39-in. ANCHORAGE

Fig. 9

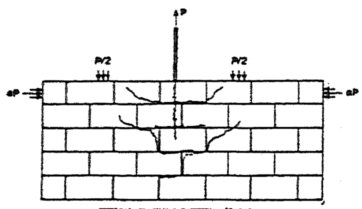

TYPICAL CRACKING PATTERN, #8 BAR

Fig. 7

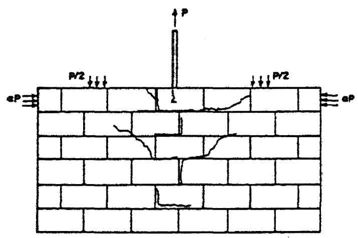

TYPICAL CRACKING PATTERN, #11 BAR

Fig. 10

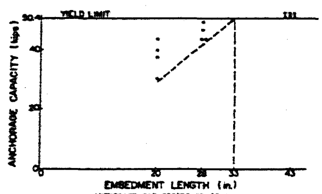

ANCHORAGE CAPACITIES OF #8 BARS

Fig. 8

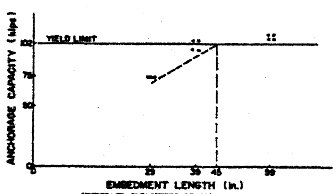

ANCHORAGE CAPACITIES OF #11 BARS

Fig. 11